PHYSICAL REVIEW D **72,** 065019 (2005)

Probing Planck scale physics with IceCube

Luis A. Anchordoqui* and Haim Goldberg†
Department of Physics, Northeastern University, Boston, Massachusetts 02115, USA

M. C. Gonzalez-Garcia‡
Y.I.T.P., SUNY at Stony Brook, Stony Brook, New York 11794-3840, USA
and IFIC, Universitat de València–C.S.I.C., Apt 22085, 46071 València, Spain

Francis Halzen§
Department of Physics, University of Wisconsin, Madison Wisconsin 53706, USA

Dan Hooper‖
Astrophysics, University of Oxford, Oxford OX1 3RH, United Kingdom

Subir Sarkar¶
Theoretical Physics, University of Oxford, Oxford OX1 3NP, United Kingdom

Thomas J. Weiler**
Department of Physics and Astronomy, Vanderbilt University, Nashville Tennessee 37235, USA
(Received 24 June 2005; published 28 September 2005)

Neutrino oscillations can be affected by decoherence induced e.g. by Planck scale suppressed interactions with the space-time foam predicted in some approaches to quantum gravity. We study the prospects for observing such effects at IceCube, using the likely flux of TeV antineutrinos from the Cygnus spiral arm. We formulate the statistical analysis for evaluating the sensitivity to quantum decoherence in the presence of the background from atmospheric neutrinos, as well as from plausible cosmic neutrino sources. We demonstrate that IceCube will improve the sensitivity to decoherence effects of $\mathcal{O}(E^2/M_{\rm Pl})$ by 17 orders of magnitude over present limits and, moreover, that it can probe decoherence effects of $\mathcal{O}(E^3/M_{\rm Pl}^2)$ which are well beyond the reach of other experiments.

DOI: 10.1103/PhysRevD.72.065019 PACS numbers: 03.65.Yz, 95.55.Vj, 95.85.Ry

I. INTRODUCTION

Despite many decades of intense effort, a satisfactory theory of quantum gravity is yet to see the light of day. Moreover, it is generally thought that the quantum effects of gravity may never be experimentally accessible because they would be manifest only at the Planck scale, $M_{\rm Pl} \equiv \sqrt{\hbar c/G_{\rm N}} \simeq 1.2 \times 10^{19}$ GeV. However, gravity, being a nonrenormalizable interaction in the language of quantum field theory, may leave a distinctive imprint at energies much lower than the Planck scale if it violates some fundamental symmetry of the effective low energy theory, akin to the violation of parity in nuclear radioactive decay at energies far below the true scale of the responsible weak interaction [1]. For example, if quantum space-time has a ''foamy'' structure in which Planck length size black holes form and evaporate on the Planck time scale, then there may be a loss of quantum information across their event horizons, providing an ''environment'' that can induce decoherence of apparently isolated matter systems [2].

The particle most sensitive to such effects would appear to be the neutrino because oscillations between neutrino flavors are a pure quantum phenomenon in which the density matrix, ρ, has the properties of a projection operator: $\mathrm{Tr}\,\rho^2 = \mathrm{Tr}\,\rho = 1$. A heuristic view of decoherence induced by interactions with the virtual black holes in the space-time foam is as follows. Since black holes are believed not to conserve global quantum numbers, neutrino flavor is randomized by interactions with the virtual black holes. The result of many interactions then is to equally populate all three possible flavors. Because black holes do conserve energy, angular momentum, and electric and color charge (unbroken gauged quantum numbers), the neutrino interacting with the virtual black hole does reemerge as a neutrino. In this connection, it has been noted already [3] that the results from the Super-Kamiokande atmospheric neutrino experiment [4] and the K2K long baseline oscillation experiment [5], interpreted in terms of a 2-generation $\nu_\mu \leftrightarrow \nu_\tau$ flavor transition, can probe decoherence effects with high sensitivity, supplementing laboratory tests based on $K^0\overline{K}^0$ oscillations and neutron interferometry [6].

*Electronic address: l.anchordoqui@neu.edu
†Electronic address: goldberg@neu.edu
‡Electronic address: concha@insti.physics.sunysb.edu
§Electronic address: halzen@pheno.physics.wisc.edu
‖Electronic address: hooper@astro.ox.ac.uk
¶Electronic address: sarkar@thphys.ox.ac.uk
**Electronic address: tom.weiler@vanderbilt.edu

It has recently been suggested [7] that antineutrinos originating in the decay of neutrons from candidate cosmic ray sources in the Galaxy [8] can provide an even more sensitive probe. The effects of quantum decoherence would alter the flavor mixture to the ratio, $\nu_e{:}\nu_\mu{:}\nu_\tau \simeq 1{:}1{:}1$, regardless of the initial flavor content. Since decoherence effects are weighted by the distance traveled by the (anti)-neutrinos, this means that if a $\overline{\nu}$ flux with ratio of flavors $\neq 1{:}1{:}1$ were to be observed from an astrophysical source, then strong constraints can be placed on the energy scale of quantum decoherence, surpassing current bounds by over 10 orders of magnitude. However if a 1:1:1 ratio is observed, this will not imply that quantum decoherence *is* responsible, since the dominant source of the (anti)neutrinos may simply not be neutron β decay. In this paper, we pursue this idea further and formulate the statistical analysis necessary for obtaining bounds on quantum decoherence from expected future detections of cosmic neutrinos.

In Sec. II, we identify a candidate neutron source in the vicinity of the Earth: Cygnus OB2. We review all existing data on the Cygnus region and show that observed directional signals at high energies [9,10] can plausibly be ascribed to a neutron source with an energy spectrum $\propto E_n^{-3.1}$. In particular, because of neutron decay, the expected anisotropy is well below limits reported by the CASA-MIA [11] and KASCADE [12] experiments. We summarize the estimate of the corresponding antineutrino flux [8]. In Sec. III, we discuss the effects of decoherence on high-energy neutrino propagation adopting the quantum dynamical semigroup formalism, where the Lindblad operators [13] describe (anti)neutrino couplings to the space-time foam. In Sec. IV, we estimate in detail the sensitivity of the IceCube detector [14] to the $\overline{\nu}$-Cygnus beam and its ability to constrain the effects of quantum decoherence. We evaluate the signal-to-noise for both track and shower events, taking into account the atmospheric neutrino background, as well as a possible contribution to the neutrino flux from the TeV γ-ray source TeV J2032+4130, recently discovered by the HEGRA experiment [15,16] in the direction of the Cygnus spiral arm. Armed with these event rates, we formulate the statistical analysis required to study the sensitivity to quantum decoherence effects. We show that IceCube can improve the sensitivity over present probes of decoherence by 4 to 17 orders of magnitude, and moreover, that it is sensitive to strongly energy dependent decoherence effects suppressed by multiple powers of the Planck scale which are beyond the reach of other experiments. Finally, in Sec. V, we confront our results with theoretical suggestions for quantum decoherence.

II. ANTINEUTRINOS FROM CYGNUS OB2

Massive star forming regions are the engines of starburst galaxies. They generate large numbers of UV photons which ionize the interstellar medium, as seen in microwave, radio, and Hα recombination line emission. They are important sources of interstellar dust heating which results in significant infrared emission. The strong winds of their massive O stars, which should pass through the Wolf-Rayet phase and explode as supernovae, release considerable amounts of kinetic energy creating a rarefied hot ($\sim 10^6$ K) superbubble that emits x rays; its cavity can eventually be discerned from observation of HI and CO lines of the interstellar gas.

Such regions are also likely sites for cosmic ray acceleration. The massive stars synthesize considerable amounts of heavy nuclei that are released either by stellar winds or during the subsequent supernova explosions. Moreover, the young stellar population can create time-correlated, clustered supernova remnants, where through cooperative acceleration processes the energy of the accelerated nuclei can be boosted above the $\sim 10^6$ GeV cutoff of individual remnants. Thus the usual Fermi mechanism might be able to accelerate cosmic rays all the way up to the ''ankle,'' where the steeply falling ($\propto E_{\rm CR}^{-3.1}$) cosmic ray spectrum flattens to $E_{\rm CR}^{-2.8}$ [17]. An immediate consequence of this nucleus-dominance picture is the *creation of free neutrons* through the photodisintegration of the nuclei on the intense ambient photon fields.

Independent evidence may be emerging for such a cosmic ray accelerator in the massive star forming region Cygnus OB2, a cluster of several thousands of hot young OB stars with a total mass of $\sim 10^4 M_\odot$ [18]. At a relatively small distance to Earth ($d \approx 1.7$ kpc), this is the largest known stellar association, with a diameter of ≈ 60 pc and a core radius of ~ 10 pc. The cluster age has been estimated [19] from isochrone fitting to be 3–4 Myr, where the age range may reflect a noncoeval star forming event. The HEGRA experiment has detected an extended TeV γ-ray source, J2032+4130, on the outer edge of Cygnus OB2 with no clear counterpart and a spectrum which can be modeled in terms of either hadronic or leptonic processes [15,16]. However the failure of Chandra and VLA to detect significant levels of x rays or radiowaves which would signal the presence of high-energy electrons [20] argues for a hadronic mechanism. Above 1 TeV, the HEGRA data can be fitted by a simple power law [16]

$$\frac{dF_\gamma}{dE_\gamma} = 6.2(\pm 1.5_{\rm stat} \pm 1.3_{\rm sys}) \times 10^{-13}\left(\frac{E_\gamma}{\rm TeV}\right)^{-1.9(\pm 0.1_{\rm stat} \pm 0.3_{\rm sys})} {\rm cm}^{-2}\,{\rm s}^{-1}\,{\rm TeV}^{-1}. \quad (1)$$

The model proposed [21] is that protons are accelerated by the collective effects of stellar winds from massive O and B stars and only the high-energy particles penetrate and interact in the innermost dense parts of the winds. The colliding protons generate π^0's which produce the observed γ rays. Convection prevents low energy protons from entering the dense wind region thus explaining the absence of MeV-GeV photons.

At very high energies ($E \gtrsim 10^{8.7}$ GeV) evidence has also been presented for neutral particles from the Cygnus spiral arm. AGASA has found a 4σ correlation of the arrival direction of cosmic rays at these energies with the Galactic Plane (GP) [22]. The GP excess, which is roughly 4% of the diffuse flux, is mostly concentrated in the direction of the Cygnus region [23]. Evidence at the 3.2σ level for a GP enhancement at similar energies has also been reported by the HiRes Collaboration [24]. The primary particles must be neutral (and stable) in order to preserve direction while propagating through the galactic magnetic field. In principle they can be photons but this is hard to reconcile with the complete isotropy observed up to $\sim 10^{7.7}$ GeV by KASCADE [25]. Intriguingly, time-dilated neutrons can reach the Earth from typical Galactic distances when their energy exceeds $\sim 10^9$ GeV so it is reasonable to ask whether these might in fact be the primaries.

The GP anisotropy is observed over the energy range $10^{8.9}$ to $10^{9.5}$ GeV. The lower threshold requires that only neutrons with energy $\gtrsim 10^9$ GeV have a boosted $c\tau_n$ sufficiently large to serve as Galactic messengers. The decay mean free path of a neutron is $c\Gamma_n\overline{\tau}_n = 9.15(E_n/10^9\ \text{GeV})$ kpc, the lifetime being boosted from its rest-frame value, $\overline{\tau}_n = 886$ seconds, to its lab value by $\Gamma_n = E_n/m_n$. Actually, the broad scale anisotropy from the direction of the GP reported by Fly's Eye [24] peaks in the energy bin $10^{8.6}$–10^9 GeV, but persists with less significance to energies as low as $10^{8.5}$ GeV. This implies that if neutrons are the carriers of the anisotropy, there *needs to be* some contribution from at least one source closer than ~ 2 kpc. Interestingly, the full Fly's Eye data includes a directional signal from the Cygnus region which was somewhat lost in unsuccessful attempts [9,10] to relate it to γ-ray emission from Cygnus X-3. As shown in Fig. 1, Cygnus OB2 is very close to the line of sight to Cygnus X-3, which is in fact ~ 8 kpc farther away than the stellar association.

The upper cutoff reflects an important feature of photodisintegration at the source: heavy nuclei with energies in the vicinity of the ankle will fragment to neutrons with energies about an order of magnitude smaller. To account for the largest neutron energies, it is necessary to continue the heavy nucleus spectrum to energies above the ankle [26]. Note that the emerging harder extragalactic spectrum will overwhelm the steeply falling galactic population at these energies. In order to fit the spectrum in the anisotropy region and maintain continuity to the ankle region without introducing a cutoff, the AGASA Collaboration required a spectrum $\propto E_n^{-3}$ or steeper [22].

In what follows, we model the neutron spectrum with a single power law reflecting the average shape of the diffuse cosmic ray spectrum between 10^6 and $10^{8.5}$ GeV, specifically:

$$\frac{dF_n}{dE_n} = \frac{dF_n}{dE_n}\bigg|_{\text{source}} e^{-d/(c\Gamma_n\overline{\tau}_n)} = CE_n^{-3.1} e^{-1/(c\Gamma_n\overline{\tau}_n)}. \quad (2)$$

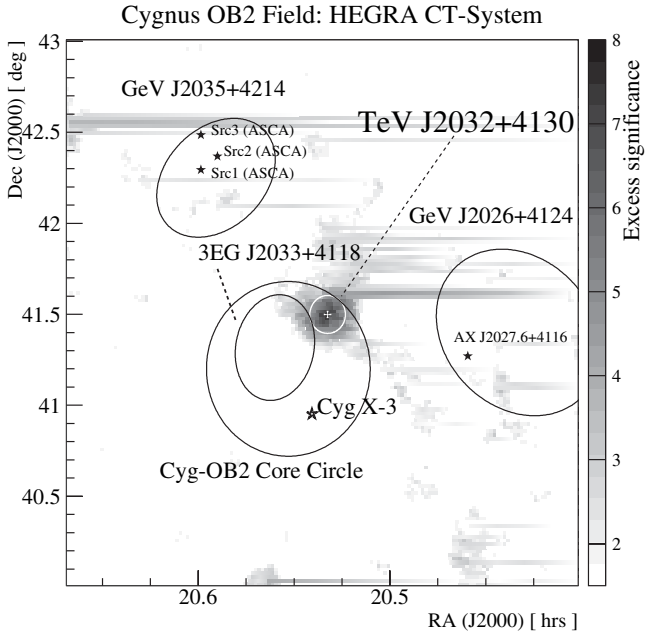

FIG. 1. Skymap of correlated event excess significance (σ) from all HEGRA IACT-System data ($3° \times 3°$ FoV) centered on the TeV source J2032+4130. Nearby objects are also shown: 95% contours for 3 EGRET sources (indicated by the ovals), their possible x ray associated counterparts (as given in Ref. [53]), and Cygnus X-3. The center of gravity with statistical errors and intrinsic size (standard deviation of a 2-dim Gaussian, σ_{src}) are indicated by the white cross and white circle, respectively. The TeV source, J2032+4130, is positioned at the edge of the error circle of the EGRET source 3EG J2033+4118, and within the core circle of the extremely dense OB stellar association Cygnus OB2 [16].

By integrating the spectrum between $E_1 = 10^{8.9}$ GeV and $E_2 = 10^{9.5}$ GeV [23], we can normalize to the observed integrated flux [23]:

$$\int_{E_1}^{E_2} CE_n^{-3.1} e^{-d/(c\Gamma_n\overline{\tau}_n)} dE_n \approx 9\ \text{km}^{-2}\,\text{yr}^{-1}, \quad (3)$$

which yields $C = 1.15 \times 10^{20}\ \text{km}^{-2}\,\text{yr}^{-1}$. We emphasize again that the neutron primaries hypothesis predicts a significant signal above the diffuse cosmic ray flux only at energies $\gtrsim 10^{8.9}$ GeV. Figure 2 shows the damping due to neutron decay which attenuates the directional signal at low energies. The predicted damped signal for a source at 1.7 kpc is well below direct limits from the CASA-MIA [11] and KASCADE [12] experiments.

For every surviving neutron at $\sim 10^9$ GeV, there are many neutrons at lower energies that do decay via $n \rightarrow p + e^- + \overline{\nu}_e$. The proton is bent by the Galactic magnetic field and the electron quickly loses energy via synchrotron radiation, but the $\overline{\nu}_e$ travels along the initial neutron direction, producing a directed TeV energy beam which is potentially observable.

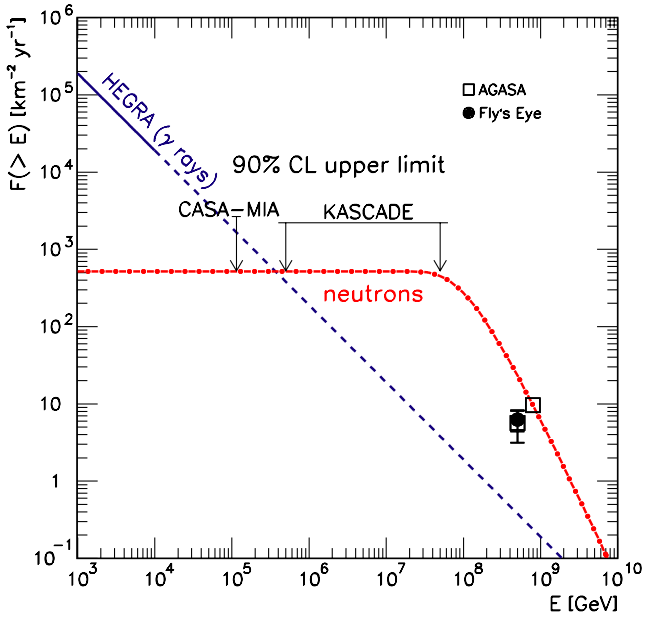

FIG. 2 (color online). The integrated neutron flux expected from Cygnus OB2 (dash-dotted line) is superimposed over the integrated fluxes observed from the Cygnus region by the Fly's Eye [9] and AGASA [10,23] experiments. Also shown is the γ-ray flux reported by the HEGRA experiment [16] and the upper limits on neutral particles derived from the CASA-MIA [11] and KASCADE [12] experiments. The solid line is a fit to the HEGRA data and the dashed line is the extrapolation to unobserved energies.

The basic formula that relates the neutron flux at the source to the antineutrino flux observed at Earth is [8]:

$$\frac{dF_{\overline{\nu}}}{dE_{\overline{\nu}}}(E_{\overline{\nu}}) = \int dE_n \frac{dF_n}{dE_n}(E_n)|_{\rm source}(1 - e^{-\frac{Dm_n}{E_n\overline{\tau}_n}}) \times \int_0^Q d\epsilon_{\overline{\nu}} \frac{dP}{d\epsilon_{\overline{\nu}}}(\epsilon_{\overline{\nu}}) \int_{-1}^{1} \frac{d\cos\overline{\theta}_{\overline{\nu}}}{2} \delta[E_{\overline{\nu}} - E_n\epsilon_{\overline{\nu}}(1 + \cos\overline{\theta}_{\overline{\nu}})/m_n]. \quad (4)$$

The variables appearing in Eq. (4) are the antineutrino and neutron energies in the lab ($E_{\overline{\nu}}$, E_n), the antineutrino angle with respect to the direction of the neutron momentum in the neutron rest frame ($\overline{\theta}_{\overline{\nu}}$), and the antineutrino energy in the neutron rest frame ($\epsilon_{\overline{\nu}}$). The last three variables are not observed by a laboratory neutrino detector, and so are integrated over. The observable $E_{\overline{\nu}}$ is held fixed. The delta function relates the neutrino energy in the lab to the three integration variables. The parameters appearing in Eq. (4) are the neutron mass and rest-frame lifetime (m_n and $\overline{\tau}_n$). Finally, $dP/d\epsilon_{\overline{\nu}}$ is the normalized probability that the decaying neutron produces an antineutrino with energy $\epsilon_{\overline{\nu}}$ in the neutron rest frame. Note that the maximum antineutrino energy in the neutron rest frame is very nearly $Q \equiv m_n - m_p - m_e = 0.71$ MeV.

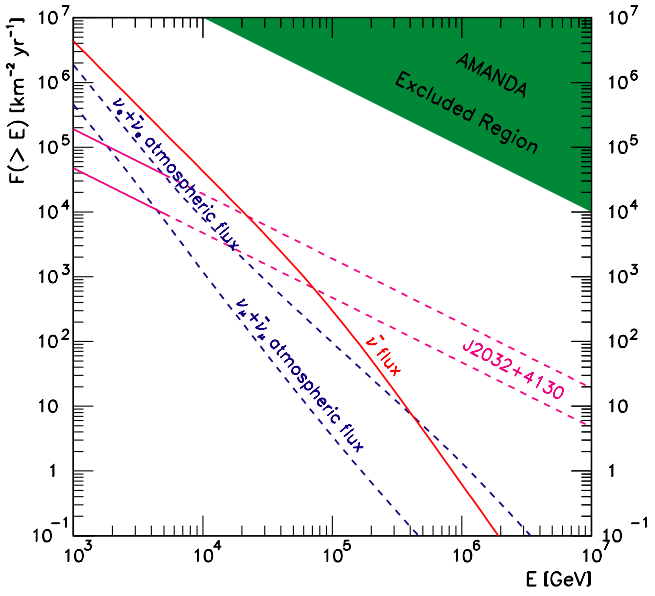

FIG. 3 (color online). Integrated flux of $\overline{\nu}_\mu + \overline{\nu}_e + \overline{\nu}_\tau$ (solid line) predicted to arrive at Earth from the direction of the Cygnus region. Also shown are the integrated $\nu_\mu + \overline{\nu}_\mu$ and $\nu_e + \overline{\nu}_e$ atmospheric fluxes for an angular bins of $1^\circ \times 1^\circ$ and $10^\circ \times 10^\circ$, respectively. The shaded band indicates the region excluded by the AMANDA experiment [54]. The fluxes of neutrinos inferred from HEGRA measurements of the γ-ray flux are also shown: the lower line is based on the assumption of $p\gamma$ interactions, whereas the upper line is based on pp interactions (the charged/neutral pion-production ratio depends on the interaction). In each case the solid portion of the line indicates the region where HEGRA data is available and the dashed part is an extrapolation to unobserved energies.

The integral neutrino flux, $F_{\overline{\nu}}(>E_{\overline{\nu}}) \equiv \int_{E_{\overline{\nu}}} dE_{\overline{\nu}}(dF_{\overline{\nu}}/dE_{\overline{\nu}})$, is particularly useful for experiments having a neutrino detection efficiency that is independent of neutrino energy, or nearly so. Our calculated integral flux, normalized to the integrated neutron flux in Eq. (3), is shown in Fig. 3. Note that the nuclear photodisintegration threshold implies an infrared cutoff on the primary neutron energy at the source, which in turn leads to a low energy cutoff of $\mathcal{O}$(TeV) on the integral flux.

III. DECOHERENCE EFFECTS IN HIGH-ENERGY NEUTRINO PROPAGATION

Even though the flux of antineutrinos produced by Cygnus OB2 is pure $\overline{\nu}_e$, the antineutrinos observed at Earth will be distributed over all flavors. This is because of neutrino oscillations, as well as possible decoherence effects induced over long distances (more on this below). In the standard treatment of neutrino oscillations, neutrino flavor eigenstates, $|\nu_\alpha\rangle$, $\alpha = e, \mu, \tau$, are expanded in terms of mass eigenstates, $|\nu_i\rangle$, $i = 1, 2, 3$, through a (unitary) matrix, U, defined by $|\nu_\alpha\rangle = \sum_{i=1}^{3} U^*_{\alpha i}|\nu_i\rangle$. This implies that the density matrix of a flavor state, ρ^α, can be ex-

pressed in terms of mass eigenstates by $\rho^\alpha = |\nu_\alpha\rangle\langle\nu_\alpha| = \sum_{i,j} U^*_{\alpha i} U_{\alpha j} |\nu_i\rangle\langle\nu_j|$. This is a pure quantum system, therefore the density matrix satisfies $\mathrm{Tr}\,\rho^2 = \mathrm{Tr}\,\rho = 1$. To get the transition amplitude, we evolve the system quantum mechanically with the Liouville equation

$$\frac{\partial \rho}{\partial t} = -i[H, \rho], \tag{5}$$

where H is the Hamiltonian of the system. For $\delta m^2_{ij} d/2E \gg 1$, the phases induced by the mass splitting, $\delta m_{ij} = m_i^2 - m_j^2$, will be erased by uncertainties in d and E, yielding for the transition probability between flavor states α and β [27]:

$$P_{\nu_\alpha \to \nu_\beta} = \mathrm{Tr}[\rho_\alpha(t)\rho_\beta] = \delta_{\alpha\beta} - 2\sum_{j>i} \mathrm{Re}(U^*_{\beta j} U_{\beta i} U_{\alpha j} U^*_{\alpha i}). \tag{6}$$

The prediction for the flavor population at Earth due to standard flavor mixing (i.e. with no space-time dynamics) of the pure $\overline{\nu}_e$ source is $\sum_j |U_{ej}|^2 |U_{\alpha j}|^2 \sim \frac{1}{3}|U_{\alpha 2}|^2 + \frac{2}{3}|U_{\alpha 1}|^2$ for flavor α, which leads to the flavor ratios $\sim$5:2:2. This is very different from the democratic 1:1:1.

The Hamiltonian evolution in Eq. (5) is a characteristic of physical systems isolated from their surroundings. The time evolution of such a quantum system is given by the continuous group of unitarity transformations, $U_t = e^{-iHt}$, where t is the time. The existence of the inverse of the infinitesimal generator, H, which is a consequence of the algebraic structure of the group, guarantees *reversibility* of the processes. For open quantum-mechanical systems, the introduction of dissipative effects lead to modifications of Eq. (5) that account for the *irreversible* nature of the evolution. The transformations responsible for the time evolution of these systems are defined by the operators of the Lindblad quantum dynamical semigroups [13]. Since this does not admit an inverse, such a family of transformations has the property of being only forward in time.

The Lindblad approach to decoherence does not require any detailed knowledge of the environment. The corresponding time evolution equation for the density matrix takes the form

$$\frac{\partial \rho}{\partial t} = -i[H_{\mathrm{eff}}, \rho] + \mathcal{D}[\rho], \tag{7}$$

where the decoherence term is given by

$$\mathcal{D}[\rho] = -\frac{1}{2}\sum_j ([b_j, \rho b_j^\dagger] + [b_j \rho, b_j^\dagger]). \tag{8}$$

Here, $H_{\mathrm{eff}} = H + H_d$ is the effective Hamiltonian of the system, H is its free Hamiltonian, H_d accounts for possible additional dissipative contributions that can be put in the Hamiltonian form, and $\{b_j\}$ is a sequence of bounded operators acting on the Hilbert space of the open quantum system, $\mathcal{H}$, and satisfying $\sum_j b_j^\dagger b_j \in \mathcal{B}(\mathcal{H})$, where $\mathcal{B}(\mathcal{H})$ indicates the space of bounded operators acting on $\mathcal{H}$.

The intrinsic coupling of a microscopic system to the space-time foam can then be interpreted as the existence of an arrow of time which in turn makes possible the connection with thermodynamics via an entropy. The monotonic increase of the von Neumann entropy, $S(\rho) = -\mathrm{Tr}(\rho \ln \rho)$, implies the Hermiticity of the Lindblad operators, $b_j = b_j^\dagger$ [28]. In addition, the conservation of the average value of the energy can be enforced by taking $[H, b_j] = 0$ [29]. The Lindblad operators of an N-level quantum-mechanical system can be expanded in a basis of matrices satisfying standard commutation relations of Lie groups. For a 3-level system, the basis comprises the eight Gell-Mann SU(3) matrices plus the 3×3 identity matrix [30].

As mentioned above, the theoretical approach provided by Lindblad quantum dynamical semigroups is very general in the sense that no explicit hypothesis has been made about the actual interactions causing the loss of coherence. Following Ref. [31], we adopt an expansion in a 3 flavor basis with a diagonal form for the 9×9 decoherence matrix, $\mathcal{D}$. Note that neutrinos oscillate among flavors separately between particle and antiparticle sectors and so the respective decoherence parameters for antineutrinos can be different from the corresponding ones in the neutrino sector. Upon averaging over the rapid oscillation for propagation between Cygnus OB2 and the Earth, only the diagonal Gell-Mann matrices survive, and so the transition probability for antineutrinos takes the form [31]:

$$P_{\overline{\nu}_\alpha \to \overline{\nu}_\beta} = \frac{1}{3} + \left[\frac{1}{2} e^{-\overline{\gamma}_3 d}(U^2_{\alpha 1} - U^2_{\alpha 2})(U^2_{\beta 1} - U^2_{\beta 2}) + \frac{1}{6} e^{-\overline{\gamma}_8 d}(U^2_{\alpha 1} + U^2_{\alpha 2} - 2U^2_{\alpha 3})(U_{\beta 1} + U^2_{\beta 2} - 2U^2_{\beta 3})\right], \tag{9}$$

where $\overline{\gamma}_3$ and $\overline{\gamma}_8$ are eigenvalues of the decoherence matrix for antineutrinos. Note that in Eq. (9) we set the *CP* violating phase to zero, so that all mixing matrix elements become real. Furthermore, under the assumptions that *CPT* is conserved and that decoherence effects are negligible at present experiments, the values of the mixing angle combinations appearing in Eq. (9) can be well determined by the usual oscillation analysis of solar, atmospheric, long-baseline (LBL) and reactor data [32]. In what follows, we will assume that *CPT* is conserved both by neutrino masses and mixing as well as in decoherence effects. Note however that since the decoherence effects in the present study primarily affect antineutrinos, our results will hold for the antineutrino decoherence parameters exclusively if *CPT* is violated only through quantum-gravity effects.

Now, we require further $\overline{\gamma}_3 = \overline{\gamma}_8 \equiv \overline{\gamma}$ ($= \gamma_3 = \gamma_8$ under *CPT* conservation) so that Eq. (9) can be rewritten

for the case of interest as

$$P_{\overline{\nu}_e\to\overline{\nu}_\mu}=P_{\overline{\nu}_\mu\to\overline{\nu}_e}=P_{\nu_e\to\nu_\mu}=P_{\nu_\mu\to\nu_e}=\frac{1}{3}+f_{\nu_e\to\nu_\mu}e^{-\overline{\gamma}d},\quad P_{\overline{\nu}_e\to\overline{\nu}_\tau}=P_{\overline{\nu}_\tau\to\overline{\nu}_e}=P_{\nu_e\to\nu_\tau}=P_{\nu_\tau\to\nu_e}=\frac{1}{3}+f_{\nu_e\to\nu_\tau}e^{-\overline{\gamma}d},$$
$$P_{\overline{\nu}_\mu\to\overline{\nu}_\tau}=P_{\overline{\nu}_\tau\to\overline{\nu}_\mu}=P_{\nu_\mu\to\nu_\tau}=P_{\nu_\tau\to\nu_\mu}=\frac{1}{3}+f_{\nu_\mu\to\nu_\tau}e^{-\overline{\gamma}d},\quad P_{\overline{\nu}_e\to\overline{\nu}_e}=P_{\nu_e\to\nu_e}=\frac{1}{3}-(f_{\nu_e\to\nu_\mu}+f_{\nu_e\to\nu_\tau})e^{-\overline{\gamma}d},\tag{10}$$
$$P_{\overline{\nu}_\mu\to\overline{\nu}_\mu}=P_{\nu_\mu\to\nu_\mu}=\frac{1}{3}-(f_{\nu_e\to\nu_\mu}+f_{\nu_\mu\to\nu_\tau})e^{-\overline{\gamma}d},\quad P_{\overline{\nu}_\tau\to\overline{\nu}_\tau}=P_{\nu_\tau\to\nu_\tau}=\frac{1}{3}-(f_{\nu_e\to\nu_\tau}+f_{\nu_\mu\to\nu_\tau})e^{-\overline{\gamma}d}.$$

We make this simplification only to emphasize the primary signature of quantum decoherence, namely, that after traveling a sufficiently long distance the flavor mixture is altered to the ratio 1:1:1, regardless of the initial flavor content. Consequently, if a flux of antineutrinos were to be observed from the Cygnus spiral arm with a flavor ratio $\neq$ 1:1:1, strong constraints can be placed on the decoherence parameter $\overline{\gamma}$.

Using the results of the up-to-date 3-ν oscillation analysis of solar, atmospheric, LBL and reactor data [32] we obtain the following values and 95% confidence ranges

$$f_{\nu_e\to\nu_\mu}=-0.106^{+0.060}_{-0.082},\qquad f_{\nu_e\to\nu_\tau}=-0.128^{+0.089}_{-0.055},$$
$$f_{\nu_\mu\to\nu_\tau}=0.057^{+0.011}_{-0.035}.\tag{11}$$

The numbers given in Eq. (11) are obtained using the same techniques as described in Ref. [32] but including the final SNO salt phase data [33].

We assume a phenomenological parametrization for the eigenvalues of the decoherence matrix [3],

$$\overline{\gamma}=\kappa_n(E_\nu/\mathrm{GeV})^n,\tag{12}$$

with the integer $n\in[-1,3]$. This allows a straightforward comparison with existing limits. Equipped with Eqs. (10)–(12), we now proceed to determine the sensitivity of IceCube to decoherence effects.

IV. SENSITIVITY REACH AT ICECUBE

In deep ice, neutrinos are detected through the observation of Čerenkov light emitted by charged particles produced in neutrino interactions. In the case of an incident high-energy muon neutrino, for instance, the neutrino interacts with a hydrogen or oxygen nucleus in the deep ice and produces a muon traveling in nearly the same direction as the neutrino. The blue Čerenkov light emitted along the muon's kilometer-long trajectory is detected by strings of PhotoMultiplier Tubes (PMTs) deployed at depth shielded from radiation. The orientation of the Čerenkov cone reveals the neutrino direction. There may also be a visible hadronic shower if the neutrino is of sufficient energy.

The Antarctic muon and neutrino-detector array (AMANDA) [34], using natural 1 mile deep Antarctic ice as a Čerenkov detector, has operated for more than three years in its final configuration: 19 strings instrumented with 680 PMTs. IceCube [14], the successor experiment to AMANDA, is now under construction. It will consist of 80 km-length strings, each instrumented with 60 PMTs spaced by 17 m. The deepest module is 2.4 km below the surface. The strings are arranged at the apexes of equilateral triangles 125 m on a side. The instrumented (not effective) detector volume is a full cubic kilometer. A surface air-shower detector, IceTop, consisting of 160 Auger-style [35] Čerenkov detectors deployed over 1 km^2 above IceCube, augments the deep-ice component by providing a tool for calibration, background rejection and air-shower physics. The expected energy resolution is ±0.1 on a $\log_{10}$ scale. Construction of the detector started in the Austral summer of 2004/2005 and will continue for 6 years, possibly less. At the time of writing, data collection by the first string has begun.

At IceCube, the events are grouped as either muon tracks or showers. Tracks include muons resulting from both cosmic muons and from charged current (CC) interaction of muon neutrinos. The angular resolution for muon tracks $\approx 0.7^\circ$ [36] allows a search window of $1^\circ\times1^\circ$. This corresponds to a search bin solid angle of $\Delta\Omega_{1^\circ\times1^\circ}\approx 3\times10^{-4}$ sr. In order to reduce the background from cosmic muons, we adopt here the quality cuts referred to as ''level 2'' cuts in Ref. [14].

In our semianalytical calculation [37], we estimate the expected number of ν_μ induced tracks from the Cygnus OB2 source antineutrino flux as

$$\mathcal{N}_S^{\mathrm{tr}}=Tn_T\int_{l'_{\min}}^{\infty}dl\int_{m_\mu}^{\infty}dE_\mu^{\mathrm{fin}}\int_{E_\mu^{\mathrm{fin}}}^{\infty}dE_\mu^0\int_{E_\mu^0}^{\infty}dE_{\overline{\nu}}\frac{dF_{\overline{\nu}_\mu}}{dE_{\overline{\nu}}}$$
$$\times(E_{\overline{\nu}})\frac{d\sigma_{\mathrm{CC}}}{dE_\mu^0}(E_{\overline{\nu}},E_\mu^0)F(E_\mu^0,E_\mu^{\mathrm{fin}},l)A_{\mathrm{eff}}^0,\tag{13}$$

where

$$\frac{dF_{\overline{\nu}_\alpha}}{dE_{\overline{\nu}}}=P_{\overline{\nu}_e\to\overline{\nu}_\alpha}(E_{\overline{\nu}})\frac{dF_{\overline{\nu}}}{dE_{\overline{\nu}}}\tag{14}$$

is the differential antineutrino flux which arrives at the Earth with flavor α after oscillation of the $\overline{\nu}_e$ in Eq. (4). Here $(d\sigma_{\mathrm{CC}}/dE_\mu^0)(E_{\overline{\nu}},E_\mu^0)$ is the differential CC interaction cross section producing a muon of energy E_μ^0, n_T is the number density of nucleons in the matter surrounding the detector, and T is the exposure time of the detector. After being produced, the muon propagates through the rock and ice surrounding the detector and loses energy. We denote by $F(E_\mu^0,E_\mu^{\mathrm{fin}},l)$ the function that represents the probability of a muon produced with energy E_μ^0, arriving at the detec-

tor with energy $E_\mu^{\rm fin}$, after traveling a distance, l. The details of the detector are encoded in the effective area, $A_{\rm eff}^0$. We use the parametrization of the $A_{\rm eff}^0$ described in Ref. [37] to simulate the response of the IceCube detector after events that are not neutrinos have been rejected (this is achieved by quality cuts referred to as ''level 2'' cuts in Ref. [14]). The minimum track length cut is $l_{\rm min} = 300$ m and we account for events with $E_\mu^{\rm fin} > 500$ GeV. With this we find that, assuming standard neutrino oscillations, one expects a total of $212 \times P_{\overline{\nu}_e \to \overline{\nu}_\mu} = 48$ $\overline{\nu}_\mu$-induced tracks from the Cygnus OB2 source in 15 years of observation.

Showers are generated by neutrino collisions—ν_e or ν_τ CC interactions, and all neutral current (NC) interactions—inside of or nearby the detector, and by muon bremsstrahlung radiation near the detector. For showers, the angular resolution is significantly worse than for muon tracks. In our analysis, we consider a shower search bin solid angle, $\Delta\Omega_{10^\circ\times 10^\circ}$. Normally, a reduction of the muon bremsstrahlung background is effected by placing a cut of 40 TeV on the minimum reconstructed energy [38]. For Cygnus OB2, this strong energy cut is not needed since this background is filtered by the Earth. Thus we account for all events with shower energy $E_{\rm sh} \geq E_{\rm sh}^{\rm min} = 1$ TeV. The directionality requirement, however, implies that the effective volume for detection of showers is reduced to the instrumented volume of the detector, 1 km^3, because of the small size of the showers (less than 200 m in radius) in this energy range.

We can now calculate the expected number of showers from the Cygnus OB2 source to be

$$\mathcal{N}_S^{\rm sh} = \mathcal{N}_S^{\rm sh,CC} + \mathcal{N}_S^{\rm sh,NC}, \tag{15}$$

where

$$\mathcal{N}_{\rm S}^{\rm sh,CC} = T n_T \mathcal{V}_{\rm eff} \int_{E_{\rm sh}^{\rm min}}^{\infty} dE_{\overline{\nu}} \sum_{\alpha=e,\tau} \frac{dF_{\overline{\nu}_\alpha}}{dE_{\overline{\nu}}}(E_{\overline{\nu}}) \sigma_{\rm CC}(E_{\overline{\nu}}), \tag{16}$$

and

$$\mathcal{N}_{\rm S}^{\rm sh,NC} = T n_T \mathcal{V}_{\rm eff} \int_{E_{\overline{\nu}} - E_{\rm sh}^{\rm min}}^{\infty} dE'_{\overline{\nu}} \int_{E_{\rm sh}^{\rm min}}^{\infty} dE_{\overline{\nu}} \sum_{\alpha=e,\mu,\tau} \frac{dF_{\overline{\nu}_\alpha}}{dE_{\overline{\nu}}} \times (E_{\overline{\nu}}) \frac{d\sigma_{\rm NC}}{dE'_{\overline{\nu}}}(E_{\overline{\nu}}, E'_{\overline{\nu}}). \tag{17}$$

Here, $(d\sigma_{\rm NC}/dE'_{\overline{\nu}})(E_{\overline{\nu}}, E'_{\overline{\nu}})$ is the differential NC interaction cross section producing a secondary antineutrino of energy, $E'_{\overline{\nu}}$. In writing Eqs. (16) and (17) we are assuming that for contained events the shower energy corresponds with the interacting $\overline{\nu}_e$ or $\overline{\nu}_\tau$ antineutrino energy ($E_{\rm sh} = E_{\overline{\nu}}$) in a CC interaction, while for NC the shower energy corresponds to the energy in the hadronic shower $E_{\rm sh} = E_{\overline{\nu}} - E'_{\overline{\nu}} \equiv E_{\overline{\nu}} y$, where y is the usual inelasticity parameter in deep inelastic scattering. In total, within the framework of standard oscillations, we expect 25 showers from the Cygnus OB2 source in 15 years of operation.

We now turn to the estimate of the background. There are two different contributions—atmospheric neutrinos and additional fluxes of extraterrestrial neutrinos. For the ''conventional'' atmospheric neutrino fluxes arising from pion and kaon decays, we adopt the 3-dimensional scheme estimates of Ref. [39], which we extrapolate to match at higher energies the 1-dimensional calculations by Volkova [40]. We also incorporate ''prompt'' neutrinos from charm decay as calculated in Ref. [41]. We obtain the number of expected track and shower events from atmospheric neutrinos as in Eqs. (13), (16), and (17) with $(dF_{\nu_\alpha}^{\rm ATM}/dE_\nu) \times (E_\nu)$ being the ν_e and ν_μ atmospheric neutrino fluxes integrated over a solid angle of $1^\circ \times 1^\circ$ (for tracks) and $10^\circ \times 10^\circ$ (for showers) width around the direction of the Cygnus OB2 source ($\theta = 131.2^\circ$). We get an expected background of 14 atmospheric tracks and 47 atmospheric showers in 15 years. Of the 47 showers, 16 correspond to ν_e CC interactions while 31 correspond to ν_μ NC interactions. The large yield of NC events is due to the fact that at these energies, the atmospheric flux contains a very unequal mix of neutrino flavors (with ratios $\approx$ 1:20:0). We have also verified that if we increase the minimum shower energy cut to 5 TeV, ν_e CC and ν_μ NC contribute in equal amounts to the number of atmospheric showers. This is in agreement with simulations by the AMANDA Collaboration [42].

We turn now to the discussion of background events from other extraterrestrial sources. As discussed in Sec. II, the TeV γ-ray flux reported by the HEGRA Collaboration [16] in the vicinity of Cygnus OB2 is likely to be due to hadronic processes: the γ rays can be directly traced to the decay π^0's produced through inelastic pp collisions [21]. Since π^0's, π^+'s, and π^-'s are produced in equal numbers, we expect two photons, two ν_e's, and four ν_μ's per π^0. On average, the photons carry one-half of the energy of the pion, and the neutrinos carry one-quarter. During propagation, the ν_μ's will partition themselves equally between ν_μ's and ν_τ's on lengths large compared to the oscillation length and so one finds at Earth a nearly identical flux for the three neutrino flavors [43]:

$$\frac{dF_{\nu_\alpha}}{dE_\nu}(E_\nu = E_\gamma/2) = 2\frac{dF_\gamma}{dE_\gamma}(E_\gamma). \tag{18}$$

For $p\gamma \to N\pi$ interactions, it can easily be shown using the Δ approximation that the resulting neutrino flux is about a factor of 4 smaller [44]. For the purposes of setting an upper bound on the neutrino flux we ignore all other sources near J2032+4130 because their steady emission in γ rays is estimated to be smaller by more over a factor of 5 than the source of interest [45]. Substituting Eq. (1) into Eq. (18) we obtain the corresponding background from neutrinos with flavor ratios 1:1:1. As can be seen in Fig. 3, the background is dominated by atmospheric neu-

trinos. Thus after 15 years of data collection we expect 18 tracks and 1 shower from J2032+4130 for standard oscillations. In summary, the directional beam from the Cygnus region provides a statistically significant signal to probe anomalous oscillations in the antineutrino sector.

We will now discuss how to isolate the possible signal due to decoherence in the antineutrinos from Cygnus OB2 from the atmospheric background and possible fluctuations in the event rate due to unknown diffuse fluxes of extraterrestrial neutrinos. In general, we can predict that the expected number of track and shower events in the direction of the Cygnus OB2 source to be

$$\mathcal{N}^{\rm tr} = \mathcal{N}^{\rm tr}_{S} + \mathcal{N}^{\rm tr}_{\rm ATM} + \mathcal{N}^{\rm tr}_{S}, \tag{19}$$

$$\mathcal{N}^{\rm sh} = \mathcal{N}^{\rm sh}_{S} + \mathcal{N}^{\rm sh}_{\rm ATM} + \mathcal{N}^{\rm sh}_{S}. \tag{20}$$

The first term corresponds to antineutrinos from neutron β decay. In the presence of decoherence effects these event rates can be computed from Eqs. (13), (16), and (17) with flavor transition probabilities given in Eq. (10) with $d = 1.7$ kpc. The second term refers to atmospheric (anti)neutrinos ($\mathcal{N}^{\rm tr}_{\rm ATM} = 14$, $\mathcal{N}^{\rm sh}_{\rm ATM} = 47$ for 15 yr of exposure). The third term takes into account additional contributions from a diffuse flux of (anti)neutrinos produced via charged pion decay. In principle, decoherence effects may also affect the expected number of events from this diffuse flux. However given that the flavor ratios both from oscillation and decoherence are very close to 1:1:1 for the case of neutrinos produced via charge pion decay, we find that there is no difference in the sensitivity region if decoherence effects are included or not in the evaluation of $\mathcal{N}^{\rm tr}_{S}$ and $\mathcal{N}^{\rm sh}_{\rm SS}$. They are normalized to the maximum expected flux from J2032+4130 by a factor $x = \mathcal{N}^{\rm tr}_{\rm SS}/18 = \mathcal{N}^{\rm sh}_{\rm SS}/1$.

Altogether, the quantities $\mathcal{N}^{\rm tr}$ and $\mathcal{N}^{\rm sh}$, as defined in Eqs. (19) and (20), can be regarded as the theoretical expectations of these events rates, corresponding to different points in the $x - \kappa_n$ parameter space. For a given set of observed rates, $\mathcal{N}^{\rm tr}_{\rm obs}$ and $\mathcal{N}^{\rm sh}_{\rm obs}$, two curves are obtained in the two-dimensional parameter space by setting $\mathcal{N}^{\rm tr}_{\rm obs} = \mathcal{N}^{\rm tr}$ and $\mathcal{N}^{\rm sh}_{\rm obs} = \mathcal{N}^{\rm sh}$. These curves intersect at a point, yielding the most probable values for the flux and decoherence scale for the given observations. Fluctuations about this point define contours of constant χ^2 in an approximation to a multi-Poisson likelihood analysis. The contours are defined by [46]

$$\chi^2 = \sum_{i}^{\rm sh,tr} 2\left[\mathcal{N}^{i} - \mathcal{N}^{i}_{\rm obs} + \mathcal{N}^{i}_{\rm obs}\ln\left(\frac{\mathcal{N}^{i}_{\rm obs}}{\mathcal{N}^{i}}\right)\right]. \tag{21}$$

As illustration, in Fig. 4 we show for the case $n = 0$, the expected constraints on κ_0 at 90, 95 and 99% C.L. for 2 d.o.f. if observations turn out to be in agreement with standard neutrino oscillation expectations, taking $\mathcal{N}^{\rm tr}_{\rm obs} = 62$ and $\mathcal{N}^{\rm sh}_{\rm obs} = 72$ (and no diffuse flux). Similar regions can be obtained for other choices of n.

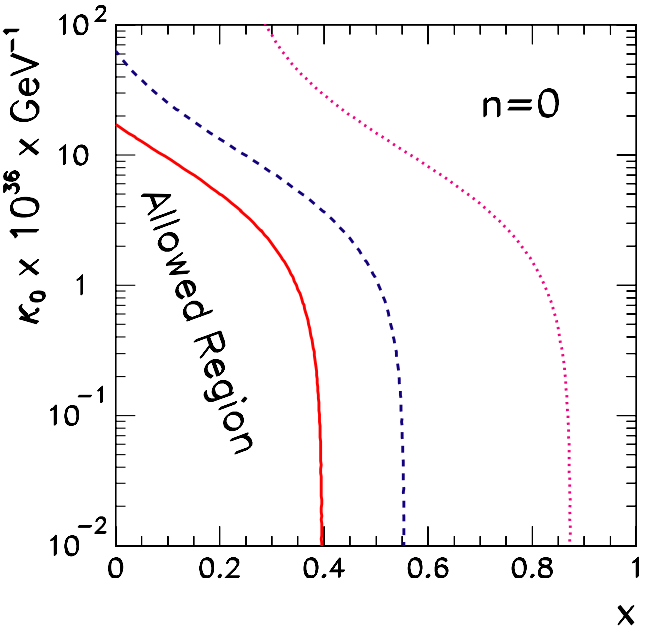

FIG. 4 (color online). IceCube's sensitivity to quantum decoherence assuming $\mathcal{N}^{\rm tr}_{\rm obs} = 62$ tracking events and $\mathcal{N}^{\rm sh}_{\rm obs} = 72$ showering events from Cygnus. The regions above and to the right of the solid, dashed and dotted lines can potentially be excluded at 90%, 95%, and 99% confidence level, respectively.

Marginalizing with respect to x, we extract the following 1 degree-of-freedom bounds on the decoherence parameters

$$\kappa_{-1} \leq 1.0 \times 10^{-34}(2.3 \times 10^{-31})\ \text{GeV}, \tag{22}$$

$$\kappa_{0} \leq 3.2 \times 10^{-36}(3.1 \times 10^{-34})\ \text{GeV}, \tag{23}$$

$$\kappa_{1} \leq 1.6 \times 10^{-40}(7.2 \times 10^{-39})\ \text{GeV}, \tag{24}$$

$$\kappa_{2} \leq 2.0 \times 10^{-44}(5.5 \times 10^{-42})\ \text{GeV}, \tag{25}$$

$$\kappa_{3} \leq 3.0 \times 10^{-47}(2.9 \times 10^{-45})\ \text{GeV}, \tag{26}$$

at 90 (99)% C.L. These should be compared with the current 90% C.L. upper limits on the decoherence parameter from the Super-Kamiokande and K2K data: $\kappa_{-1} \leq 2.0 \times 10^{-21}$ GeV, $\kappa_0 \leq 3.5 \times 10^{-23}$ GeV and $\kappa_2 \leq 9.0 \times 10^{-28}$ GeV [3]. It is clear that IceCube will provide a major improvement in sensitivity to the possible effects of quantum gravity.

V. DISCUSSION

Having demonstrated that IceCube will be able to set bounds on quantum decoherence effects well beyond the levels currently probed, we now comment briefly on the theoretical implications.

Any type of high-energy/short distance space-time foam interaction given in Eq. (9) can be understood in analogy with the tracing out of the degrees of freedom of a thermal bath (with temperature T) with which the open system (in our case a neutrino beam) interacts. A simple version of the interaction with the bath can be written as $H_{\rm int} = \sum_j b_j(a + a^\dagger)$, where $a, a^\dagger$ are raising and lowering operators for space-time foam excitations, with $\langle a^\dagger a\rangle = (e^{E_{\rm bath}/T} - 1)^{-1}$ [47].

The energy behavior of $\overline{\gamma}$ depends on the dimensionality of the operators b_j. But care must be taken, since $\mathcal{D}$ is bilinear in the b_j, and due to the Hermiticity requirement, each b_j is itself at least bilinear in the neutrino fields ψ. Examples are

$$b_j \propto \int d^3x \psi^\dagger (i\partial_t)^j \psi, \tag{27}$$

where $j = 0, 1, 2\ldots$. A Fourier expansion of the fields $\psi, \psi^\dagger$, inserted into Eq. (27), gives the energy behavior $b_j \propto E_{\overline{\nu}}^j$, and hence $\overline{\gamma} \propto E_{\overline{\nu}}^{2j}$. This restriction of the energy behavior to nonnegative even powers of $E_{\overline{\nu}}$ may possibly be relaxed when the dissipative term is directly calculated in the most general space-time foam background.

An interesting example is the case where the dissipative term is dominated by the dimension-4 operator b_1, $\int d^3x \psi^\dagger i\partial_t \psi$, yielding the energy dependence $\overline{\gamma} \propto E_{\overline{\nu}}^2/M_{\rm Pl}$. This is characteristic of noncritical string theories where the space-time defects of the quantum gravitational environment are taken as recoiling D branes, which generate a cellular structure in the space-time manifold [48].

Although the cubic energy dependence $\overline{\gamma} \propto E_{\overline{\nu}}^3$ is not obtainable from the simple operator analysis presented above, it may be heuristically supported by a general argument that each of the b_j must be suppressed by at least one power of $M_{\rm Pl}$, giving a leading behavior

$$\overline{\gamma} = \tilde{\kappa} E_{\overline{\nu}}^3/M_{\rm Pl}^2. \tag{28}$$

Here $\tilde{\kappa}$ is a dimensionless parameter which by naturalness is expected to be $\mathcal{O}(1)$. Decoherence effects with this energy behavior are undetectable by existing experiments. However, since the loss of quantum coherence is weighted by the distance traveled by the antineutrinos, by measuring the $\overline{\nu}$-Cygnus beam IceCube will attain a sensitivity down to $\tilde{\kappa} \lesssim 3.0 \times 10^{-7}$ at 99% C.L., well below the natural expectation.

Finally, we note an interesting aspect of the κ_{-1} limit. For $n = -1$, a nonvanishing $\overline{\gamma}$ in Eq. (10) can be related to a finite $\overline{\nu}_e$ lifetime in the lab system [49]:

$$e^{-\overline{\gamma} d} \equiv e^{-d/\tau_{\rm lab}} = e^{-d m_{\overline{\nu}_e}/E_{\overline{\nu}} \overline{\tau}_{\overline{\nu}_e}}, \tag{29}$$

where $\overline{\tau}_{\overline{\nu}_e}$ is the antineutrino rest-frame lifetime and $m_{\overline{\nu}_e}$ its mass. Therefore the 90% bound from IceCube on κ_{-1} can be translated into

$$\frac{\overline{\tau}_{\overline{\nu}_e}}{m_{\overline{\nu}_e}} > 10^{34}\ {\rm GeV}^{-2} \equiv 6.5\ {\rm s\,eV}^{-1}. \tag{30}$$

This corresponds to an improvement of about 4 orders of magnitude over the best existing bounds from solar neutrino data [50], and of course gives results comparable to the reach derived previously for neutrinos decaying over cosmic distances [51]. It should be noted that although the similar algebraic structure of the decoherence term in Eq. (10) and a decaying component in the neutrino beam provide a bound on the neutrino lifetime, these are conceptually two different processes. The decoherence case can be viewed as a successive absorption and reemission of a neutrino from the quantum foam with change in flavor but no change in the average energy because of the condition $[H, b_j] = 0$. This contrasts with the decay process which involves the emission of an additional particle.

In conclusion, the IceCube experiment will be sensitive to the effects of quantum decoherence at a level well beyond current limits. In particular, antineutrinos produced in the decays of neutrons from Cygnus OB2 provide an excellent source in which to search for such effects [52]. Although the precise conclusions depend on the model considered, we find that in general IceCube can achieve a sensitivity of more than 10 orders of magnitude beyond current bounds on decoherence through observations of Galactic sources of neutrons.

ACKNOWLEDGMENTS

We would like to thank Felix Aharonian, Gavin Rowell, and the HEGRA Collaboration for permission to reproduce Fig. 1. L. A. A. and H. G. are supported by the U.S. National Science Foundation (NSF) Grants No. PHY-0457004 and No. PHY-0244507, respectively. MCG-G is supported by the U.S. NSF Grant No. PHY0354776 and by Spanish Grants No. FPA-2004-00996 and No. GRUPOS03/013. F. H. is supported in part by the U.S. NSF under Grant No. OPP- 0236449, in part by the U.S. Department of Energy (DoE) Grant No. DE-FG02-95ER40896, and in part by the University of Wisconsin Research Committee with funds granted by the Wisconsin Alumni Research Foundation. D. H. is supported by the Leverhulme trust. S. S. is supported by PPARC. T. J. W. is supported by the DoE DE-FG05-85ER40226 and NASA-ATP 02-000-0151 in the USA, and by the Center for Fundamental Physics (CfFP) at CCLRC Rutherford-Appleton Laboratory, U.K.

[1] For reviews, see S. Sarkar, Mod. Phys. Lett. A **17**, 1025 (2002); **17**, 1025 (2002); L. Smolin, hep-th/0303185; F. W. Stecker, New Astron. Rev. **48**, 437 (2004); G. Amelino-Camelia, C. Lammerzahl, A. Macias, and H. Muller, AIP Conf. Proc. **758**, 30 (2005).

[2] S. W. Hawking, Commun. Math. Phys. **87**, 395 (1982); for a review, see L. J. Garay, Int. J. Mod. Phys. A **14**, 4079 (1999).

[3] E. Lisi, A. Marrone, and D. Montanino, Phys. Rev. Lett. **85**, 1166 (2000); G. L. Fogli, E. Lisi, A. Marrone, and D. Montanino, Phys. Rev. D **67**, 093006 (2003).

[4] Y. Fukuda *et al.* (Super-Kamiokande Collaboration), Phys. Rev. Lett. **81**, 1562 (1998).

[5] M. H. Ahn *et al.* (K2K Collaboration), Phys. Rev. Lett. **90**, 041801 (2003).

[6] J. R. Ellis, J. S. Hagelin, D. V. Nanopoulos, and M. Srednicki, Nucl. Phys. B **241**, 381 (1984); J. Bernabeu, N. E. Mavromatos, J. Papavassiliou, and A. Waldron-Lauda, hep-ph/0506025 [Phys. Rev. D (to be published).]

[7] D. Hooper, D. Morgan, and E. Winstanley, Phys. Lett. B **609**, 206 (2005); D. Hooper, D. Morgan, and E. Winstanley, hep-ph/0506091.

[8] L. A. Anchordoqui, H. Goldberg, F. Halzen, and T. J. Weiler, Phys. Lett. B **593**, 42 (2004).

[9] G. L. Cassiday *et al.*, Phys. Rev. Lett. **62**, 383 (1989).

[10] M. Teshima *et al.*, Phys. Rev. Lett. **64**, 1628 (1990).

[11] A. Borione *et al.* (CASA-MIA Collaboration), Phys. Rev. D **55**, 1714 (1997).

[12] G. Maier *et al.*, in Proceedings of the 28th International Cosmic Ray Conference, Tsukuba, Japan, 2003.

[13] G. Lindblad, Commun. Math. Phys. **48**, 119 (1976).

[14] J. Ahrens *et al.* (IceCube Collaboration), Astropart. Phys. **20**, 507 (2004).

[15] F. A. Aharonian, A. Akhperjanian, M. Beilicke, Y. Uchiyama, and T. Takahashi, Astron. Astrophys. **393**, L37 (2002).

[16] F. Aharonian *et al.* (HEGRA Collaboration), astro-ph/0501667.

[17] L. Anchordoqui, T. Paul, S. Reucroft, and J. Swain, Int. J. Mod. Phys. A **18**, 2229 (2003).

[18] J. Knodlseder, astro-ph/0007442.

[19] J. Knodlseder, M. Cervino, J. M. L. Duigou, G. Meynet, D. Schaerer, and P. von Ballmoos, Astron. Astrophys. **390**, 945 (2002).

[20] Y. Butt *et al.*, Astrophys. J. **597**, 494 (2003).

[21] D. F. Torres, E. Domingo-Santamaria, and G. E. Romero, Astrophys. J. **601**, L75 (2004).

[22] N. Hayashida *et al.* (AGASA Collaboration), Astropart. Phys. **10**, 303 (1999).

[23] M. Teshima *et al.*, in *Proceedings of the 27th International Cosmic Ray Conference* (Copernicus Gesellschaft, 2001) p. 341.

[24] D. J. Bird *et al.* (HIRES Collaboration), Astrophys. J. **511**, 739 (1999).

[25] T. Antoni *et al.* (KASCADE Collaboration), Astrophys. J. **604**, 687 (2004).

[26] To produce the highest energy neutrons (with energy $\lesssim 10^{9.2}$ GeV) via photodisintegration of medium mass (say, $A = 10$–20) nuclei, one needs primary particles with energies $\lesssim 10^{10.2}$ GeV. For a falling spectrum $\propto E_{\rm CR}^{-3}$, the medium mass nucleus population at $10^{10.2}$ GeV is roughly 3 orders of magnitude smaller than the diffuse flux at $10^{9.2}$ GeV. This means that it is about 1.6 orders of magnitude smaller than the reported cosmic ray excess. However, since each nucleus produces roughly A–Z neutrons, the average number of liberated neutrons is on the same order of magnitude, $1.6 - \log_{10}(A–Z)$, than the observed neutron population at $\lesssim 10^{9.2}$ GeV.

[27] J. G. Learned and S. Pakvasa, Astropart. Phys. **3**, 267 (1995).

[28] F. Benatti and H. Narnhofer, Lett. Math. Phys. **15**, 325 (1988).

[29] T. Banks, L. Susskind, and M. E. Peskin, Nucl. Phys. B **244**, 125 (1984); J. Liu, hep-th/9301082.

[30] A particular subclass of Lindblad operators satisfying $b_j = \lambda_j H$ (where λ_j are c-number constants) ensures that the purity of state vectors is preserved during evolution: S. L. Adler, Phys. Rev. D **62**, 117901 (2000). In this paper we do not consider this kind of energy dissipation, but rather dissipative effects where the evolution operators are able to transform a pure state into a mixed one.

[31] A. M. Gago, E. M. Santos, W. J. C. Teves, and R. Zukanovich Funchal, hep-ph/0208166.

[32] M. C. Gonzalez-Garcia, hep-ph/0410030.

[33] K. Miknaitis *et al.* (SNO Collaboration), hep-ex/0505071.

[34] E. Andres *et al.* (AMANDA Collaboration), Astropart. Phys. **13**, 1 (2000).

[35] J. Abraham *et al.* (Auger Collaboration), Nucl. Instrum. Methods Phys. Res., Sect. A **523**, 50 (2004).

[36] J. Ahrens *et al.* (IceCube Collaboration), Nucl. Phys. B Proc. Suppl. **118**, 388 (2003).

[37] M. C. Gonzalez-Garcia, F. Halzen, and M. Maltoni, Phys. Rev. D **71**, 093010 (2005).

[38] M. Ackermann (AMANDA Collaboration), Astropart. Phys. **22**, 127 (2004).

[39] M. Honda, T. Kajita, K. Kasahara, and S. Midorikawa, Phys. Rev. D **70**, 043008 (2004).

[40] L. V. Volkova, Sov. J. Nucl. Phys. **31**, 784 (1980) [Yad. Fiz. **31**, 1510 (1980)].

[41] P. Gondolo, G. Ingelman, and M. Thunman, Astropart. Phys. **5**, 309 (1996).

[42] J. Ahrens *et al.* (AMANDA Collaboration), Phys. Rev. D **67**, 012003 (2003).

[43] L. A. Anchordoqui, H. Goldberg, F. Halzen, and T. J. Weiler, Phys. Lett. B **600**, 202 (2004).

[44] L. A. Anchordoqui, H. Goldberg, F. Halzen, and T. J. Weiler, Phys. Lett. B **621**, 18 (2005); M. Ahlers, L. A. Anchordoqui, H. Goldberg, F. Halzen, A. Ringwald, and T. J. Weiler, Phys. Rev. D **72**, 023001 (2005).

[45] This includes the famous microquasar Cygnus X-3, for which HEGRA Collaboration reported [16] an upper limit an upper limit for steady emission of $F_\gamma(E_\gamma > 0.7\ \text{TeV}) = 1.7 \times 10^{-13}\ \text{cm}^{-2}\,\text{s}^{-1}$.

[46] S. Baker and R. D. Cousins, Nucl. Instrum. Methods Phys. Res., Sect. A **221**, 437 (1984).

[47] A. S. Davydov, *Quantum Mechanics* (Pergamon Press, 1976), 2nd ed., p. 438.

[48] J. R. Ellis, N. E. Mavromatos, D. V. Nanopoulos, and E. Winstanley, Mod. Phys. Lett. A **12**, 243 (1997); J. R. Ellis, N. E. Mavromatos, and D. V. Nanopoulos, Mod. Phys. Lett. A **12**, 1759 (1997).

[49] V. D. Barger, J. G. Learned, S. Pakvasa, and T. J. Weiler,

Phys. Rev. Lett. **82**, 2640 (1999).
[50] J. F. Beacom and N. F. Bell, Phys. Rev. D **65**, 113009 (2002).
[51] J. F. Beacom, N. F. Bell, D. Hooper, S. Pakvasa, and T. J. Weiler, Phys. Rev. Lett. **90**, 181301 (2003).
[52] There are other possible candidate sources for antineutrinos from neutron β decay, such as the Orion OB association at $\sim$450 pc from Earth [C. Briceno, N. Calvet, J. Hernandez, A. K. Vivas, L. Hartmann, J. J. Downes, and P. Berlind, astro-ph/0410521], and the Gould belt at 200 pc [N. Gehrels, D. J. Macomb, D. L. Bertsch, D. J. Thompson, and R. C. Hartman, Nature (London) **404** , 363 (2000)]. These may not however achieve the cooperative acceleration mechanism necessary for emitting neutrons with sufficient energy to reach us without decay and thus may constitute unidentified sources in the IceCube ν_μ data set. However, the simultaneous observation of showers in the same angular bin, with ratio to tracks close to that expected from neutron β decay, would allow identification of a cosmic ray source even without direct observation of a neutron excess.
[53] M. S. E. Roberts, R. W. Romani, and N. Kawai, Astrophys. J. Suppl. Ser. **133**, 451 (2001).
[54] J. Ahrens (AMANDA Collaboration), Phys. Rev. Lett. **92**, 071102 (2004).